




SOLARIS National Synchrotron Radiation Centre in Krakow, Poland

Jakub Szlachetko^{1,a}, Jacek Szade¹, Edyta Beyer¹ , Wojciech Błachucki², Piotr Ciochoń¹, Paul Dumas³, Kinga Freindl⁴, Grzegorz Gazdowicz¹, Sebastian Glatt⁵, Krzysztof Guła¹, Josef Hormes^{6,7}, Paulina Indyka¹, Agnieszka Klonecka^{1,8}, Jacek Kołodziej^{1,8}, Tomasz Kołodziej¹, Józef Korecki⁴, Paweł Korecki^{1,8}, Filip Kosiorowski⁹, Karolina Kosowska¹, Grzegorz Kowalski¹, Maciej Kozak^{1,10}, Paulina Koziol^{1,8}, Wojciech Kwiatek², Danuta Liberda¹, Henning Lichtenberg¹¹, Ewa Madej⁴, Anna Mandziak¹, Andrzej Marendziak¹, Krzysztof Matlak¹, Alexey Maximenko¹, Paweł Nita^{1,8}, Natalia Olszowska¹, Roman Panaś¹, Ewa Partyka-Jankowska¹, Marcel Piszak¹, Alexander Prange^{7,11}, Michał Rawski^{1,5}, Maciej Roman¹, Marcin Rosmus¹, Marcin Sikora¹², Joanna Sławek¹, Tomasz Sobol¹, Katarzyna Sowa¹, Nika Spiridis⁴, Joanna Stępień¹², Magdalena Szczepanik¹, Michał Ślęzak⁹, Tomasz Ślęzak⁹, Tolek Tyliczak¹, Grzegorz Ważny¹, Jarosław Wiechecki¹, Dorota Wilgocka-Ślęzak⁴, Barbara Wolanin¹, Paweł Wróbel⁹, Tomasz Wróbel¹, Marcin Zajac¹, Adriana Wawrzyniak^{1,b}, Marek Stankiewicz^{1,c}

¹ SOLARIS National Synchrotron Radiation Centre, Jagiellonian University, Krakow, Poland

² Institute of Nuclear Physics Polish Academy of Sciences, Krakow, Poland

³ SMIS Beamline, SOLEIL Synchrotron, L'orme Des Merisiers, Gif sur Yvette, France

⁴ Jerzy Haber Institute of Catalysis and Surface Chemistry Polish Academy of Sciences, Krakow, Poland

⁵ Malopolska Centre of Biotechnology, Jagiellonian University, Krakow, Poland

⁶ Institute of Physics, Rheinische Friedrich-Wilhelm-University, Bonn, Germany

⁷ Center for Advanced Microstructures and Devices, Louisiana State University, Baton Rouge, USA

⁸ Faculty of Physics, Astronomy and Applied Computer Science, Jagiellonian University, Krakow, Poland

⁹ Faculty of Physics and Applied Computer Science, AGH University of Science and Technology, Krakow, Poland

¹⁰ Faculty of Physics, Adam Mickiewicz University, Poznań, Poland

¹¹ Hochschule Niederrhein University of Applied Sciences, Krefeld, Germany

¹² Academic Centre for Materials and Nanotechnology, AGH University of Science and Technology, Krakow, Poland

Received: 26 July 2022 / Accepted: 12 December 2022

© The Author(s) 2023, corrected publication 2023

Abstract The SOLARIS synchrotron located in Krakow, Poland, is a third-generation light source operating at medium electron energy. The first synchrotron light was observed in 2015, and the consequent development of infrastructure lead to the first users' experiments at soft X-ray energies in 2018. Presently, SOLARIS expands its operation towards hard X-rays with continuous developments of the beamlines and concurrent infrastructure. In the following, we will summarize the SOLARIS synchrotron design, and describe the beamlines and research infrastructure together with the main performance parameters, upgrade, and development plans.

1 Introduction to the facility

The SOLARIS National Synchrotron Research Centre is a modern and extensive multidisciplinary research infrastructure operating since 2015 in Krakow, Poland. Its outstanding capabilities place it at the cutting edge of low-energy facilities in the world. It was created as a result of an unprecedented collaboration between Jagiellonian University and the MAX IV Laboratory, a research facility in Lund, Sweden. The SOLARIS synchrotron is composed of a 600 MeV linear accelerator (linac) with a radio frequency (RF) thermionic gun as an electron source and a vertical transfer line that is used as an injector to the storage ring [1]. The storage ring with a circumference of 96 m and 1.5 GeV maximum energy (see Fig. 1) consists of 12 Double-Bend Achromat (DBA) cells, two 100 MHz main RF cavities, and two passive 3rd harmonic cavities, injection septum and dipole kicker, diagnostics and vacuum systems. The technology used allows obtaining a low-emittance (6 nm rad) machine, and its compact design allows one to accommodate up to 10

Focus Point on Accelerator-based Photon Science Strategy, Prospects and Roadmap in Europe: a Forward View to 2030. Guest editors: R. Abela, T. Tschentscher, J. Susini, G. García.

^a e-mail: jakub.szlachetko@uj.edu.pl (corresponding author)

^b e-mail: adriana.wawrzyniak@uj.edu.pl (corresponding author)

^c e-mail: marek.stankiewicz@uj.edu.pl (corresponding author)

Fig. 1 The layout of SOLARIS accelerators with main parameters

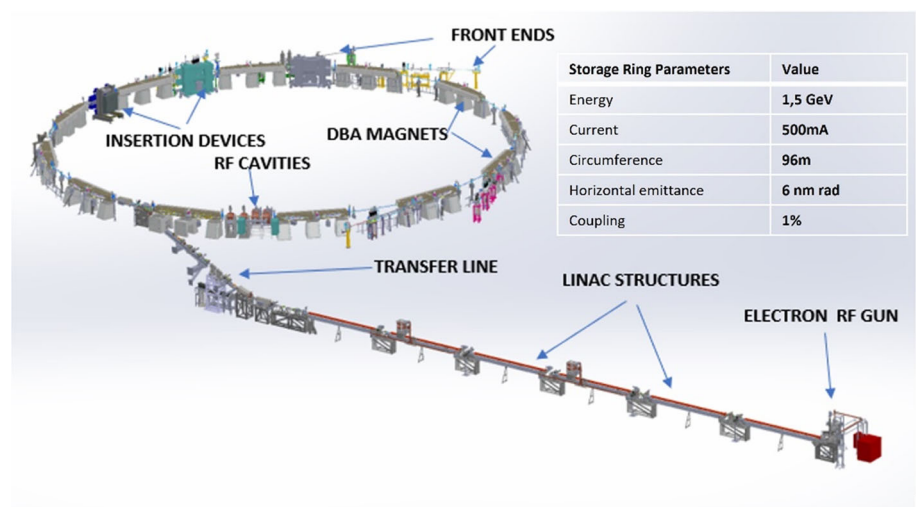
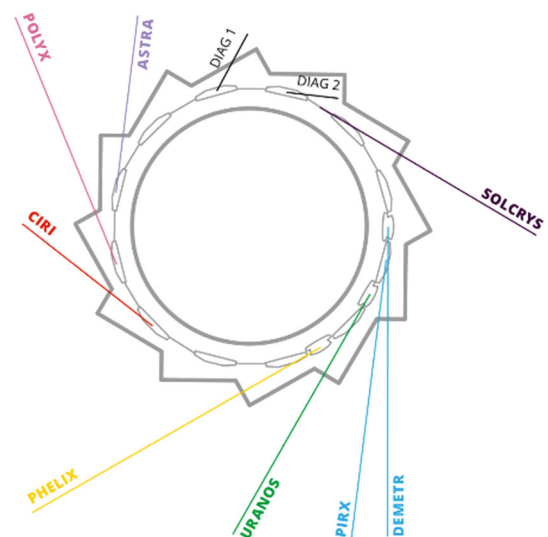


Fig. 2 Schematic overview of the SOLARIS beamlines



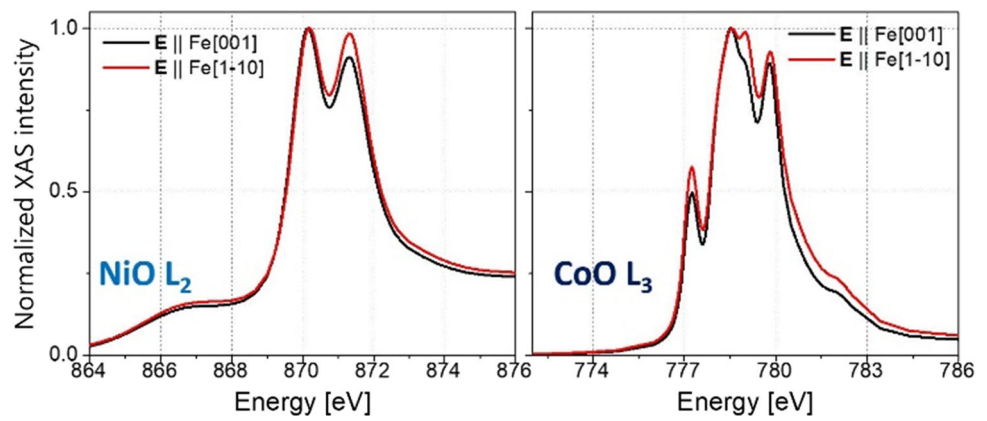
relatively long (~2.5 m) insertion devices (IDs) in straight sections [2, 3]. The main components and parameters of the SOLARIS accelerator infrastructure storage ring are shown in Fig. 1.

Since October 2018 the SOLARIS synchrotron is delivering beam to users. The storage ring operates at a final energy of 1.5 GeV in a decay mode with a maximum current of 500 mA and a total lifetime of 15 h [3]. Since 2018, high beam availability above 90% is maintained, and in 2021, 4654 h of total beamtime was scheduled. The injection to the storage ring is done twice per day, and 22 h/day of beam time is declared for users. The early stage of SOLARIS Centre development has been reported previously in [4]. Presently, SOLARIS Centre delivers experiments with five beamlines (overall six end-stations) and a cryo-microscopes facility, while three additional beamlines are under construction and several more are in conceptual preparations. A schematic overview of these is shown in Fig. 2. SOLARIS has over 1000 registered users and presently delivers over 100 experiments per year for user operation.

2 Present status and scientific highlights

The SOLARIS National Synchrotron Radiation Centre currently operates beamlines at photon energies ranging from VUV to hard X-rays and provides different photon- and electron-based techniques for sample investigations. The PIRX beamline (Premiere InfRastructure for Xas) is designed to cover the soft X-ray energy range from a bending magnet source and by using a plane grating monochromator and other optics to transfer radiation into moderate intense infrastructure dedicated to absorption spectroscopy techniques, allowing for both electron and X-ray fluorescence detection [5]. The beamline is co-operated by Jagiellonian University, the Jerzy Haber Institute of Catalysis and Surface Chemistry of the Polish Academy of Sciences, and the AGH University of Science and Technology in Kraków. The end-station with an electromagnet and liquid helium cryostat can be used for many applications

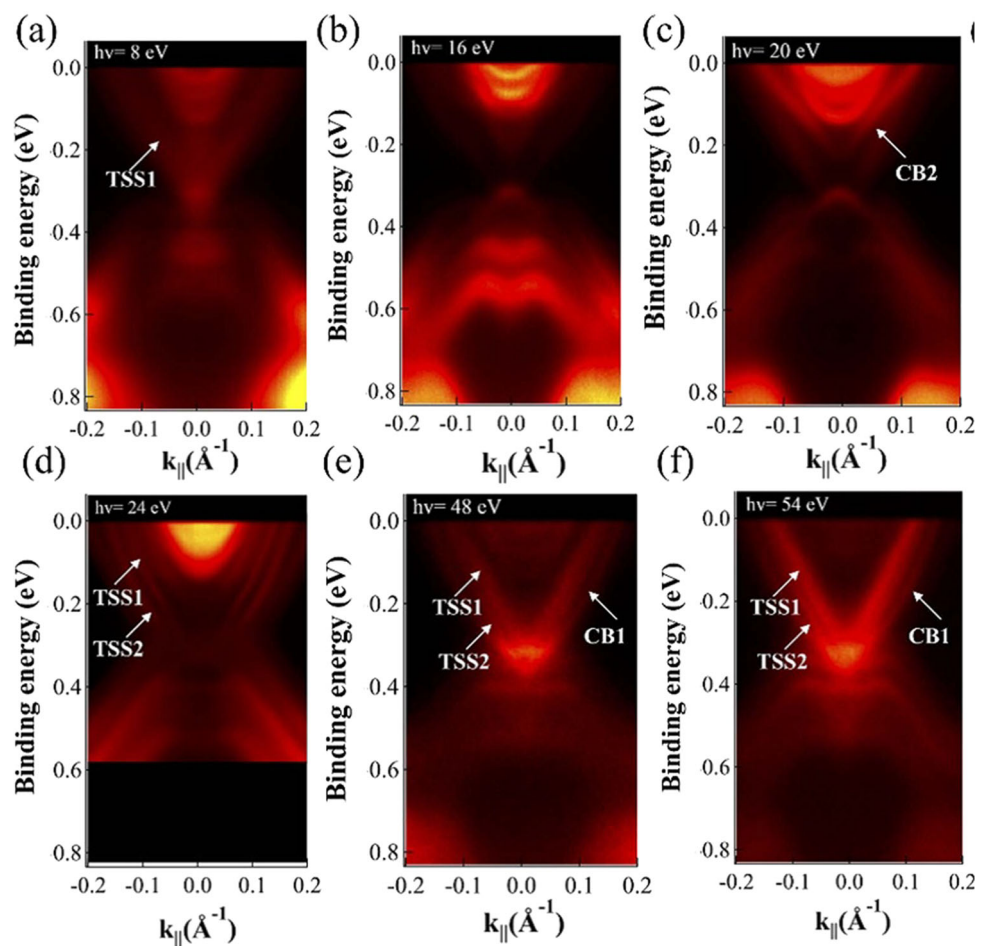
Fig. 3 Exemplary XAS spectra as measured with linearly polarized X-ray beam for both NiO (111) (left panel) and CoO(111) (right panel) antiferromagnetic films epitaxially grown on Fe(110)/W(110). The direction of the incoming X-rays is parallel to the sample normal and its linear polarization is parallel either to the Fe[1–10] or to Fe[001] in-plane direction



including material science, surface physics, magnetism, and biological systems. The most successful projects were focused on charge storage materials related to Li- or Na-based batteries [6], superconductors [7], and magnetism of the multilayer systems [8–13]. In Fig. 3, we show exemplary X-ray absorption spectra (XAS) as measured with linearly polarized X-ray beam for both NiO(111) (left panel) and CoO(111) (right panel) antiferromagnetic films epitaxially grown on Fe(110)/W(110). In both cases, spectra collected for two in-plane orthogonal orientations of electric field vector differ strongly which means that large X-ray magnetic linear dichroism (XMLD) effect is documented. Systematic studies prove that in both studied cases ferromagnetic sublayer plays a dominant role and determines the magnetic state of the neighbouring antiferromagnet (AFM); however, different interaction mechanisms are involved. In CoO/Fe bilayers, the AFM spins are frozen and their orientation is imprinted by magnetization of the Fe layer when the system passes the Neel temperature of CoO [7, 9]. For NiO/Fe bilayers, the AFM spins are rotatable and always follow the reorientation of Fe magnetization, which can be controlled by an external magnetic field or via the temperature and thickness-driven spin reorientation transition of Fe(110). In a NiO(111)/Fe(110) system of uniform thickness, two magnetic states with orthogonal spin orientations can be stabilized in NiO AFM and field-free, reversible switching between these two AFM states was demonstrated [10, 11]. The URANOS beamline (Ultra Resolved ANgular phOtoelectron Spectroscopy beamline) is dedicated to material sciences and enables measurements in the energy range from 8 to 170 eV for ARPES measurements and up to 500 eV for XPS measurements. It enables measurements with high-energy resolution (total resolution < 10 meV for energy < 40 eV and temperatures < 20 K) and angular resolution (< 0.1°). The source of electromagnetic radiation is the Apple II elliptically polarizing undulator (EPU), and the beamline is equipped with two monochromators: a plane grating monochromator (PGM) and a normal incidence monochromator (NIM). The cryogenic 5-axis manipulator enables rotation in large ranges of angles, and the temperature stabilization on the sample is in the range from 6.5 to 500 K. In particular, from several possible studies, magnetic topological insulators (MTIs) were intensively researched because they represent a possible route towards manipulating quantum information, coherent spin transport, and high-efficiency catalysis [14]. In the last years, URANOS research groups have tried to understand the phenomena in magnetic MTI, concentrated on studying both the magnetism of topological insulator crystals with ferromagnetic dopants in bulk [15, 16], surface magnetism on a topological insulator realized by ferromagnetic monolayer [17], the magnetism of self-organizing ferromagnetic layers separated by layers of a topological insulator which can generate FM or AFM order [18, 19] and axion physics [14]. Particularly important are studies on the organization of FM layers that generate intrinsic antiferromagnetic topological insulators in bulk in the compounds $\text{MnBi}_2\text{Te}_4/(\text{Bi}_2\text{Te}_3)_n$. Sitnicka et al. [18] showed that compiling structural and magnetic metrics of disorder in ferromagnetic (FM) $\text{MnBi}_2\text{Te}_4/(\text{Bi}_2\text{Te}_3)_n$ leads to migration of Mn between MnBi_2Te_4 layers and otherwise non-magnetic Bi_2Te_3 layers and induces FM coupling of Mn-depleted MnBi_2Te_4 with Mn-doped Bi_2Te_3 . Angle-resolved photoemission spectroscopy and density functional theory studies show that Mn disorder causes delocalization of electron wave functions and a change of the surface band structure compared to the ideal $\text{MnBi}_2\text{Te}_4/(\text{Bi}_2\text{Te}_3)_n$ (Fig. 4). These findings highlight the critical importance of disorder in achieving new quantum anomalous Hall platforms, as well as exploring novel axion physics in intrinsic topological magnets [18].

The PHELIX beamline has been operational since 2019 and covers a soft X-ray energy range of radiation. It enables to unveil the electronic properties of investigated materials owing to a variety of complementary spectroscopic measurements under ultra-high vacuum conditions, offering different preparation options [20]. The source of the radiation is an elliptically polarizing undulator giving variable polarization and exceptionally bright light compared to conventional X-ray sources. The available photon energy range (50–1500 eV) matches the excitation and absorption energies of elements present in the vast majority of materials used in state-of-the-art electronic devices [21], modern catalysts [22], or fuel cells [23]. The heart of the PHELIX analysis chamber is an electrostatic hemispherical analyser with an electron deflection mode (scanned angle lens–SAL) enabling angle-resolved photoelectron spectroscopy measurements. The energy resolution is limited by the resolving power of the diffraction gratings which equals 10, 000. The analyser is combined with a FERRUM 2D VLEED spin detector. The end-station provides an opportunity to measure angle integrated photoelectron spectra. By adjusting the photon energy to specific features at the absorption edges of different elements, XPS spectra in resonant mode might be collected. In particular, PHELIX offers a unique opportunity to

Fig. 4 Surface electronic band structure of $\text{MnBi}_2\text{Te}_4/(\text{Bi}_2\text{Te}_3)_n$. (a–f) ARPES data of the disordered $\text{MnBi}_2\text{Te}_4/(\text{Bi}_2\text{Te}_3)_n$ (sample S3) obtained along $\Gamma \rightarrow \bar{M}$ direction at photon energies 8 eV, 16 eV, 20 eV, 24 eV, 48 eV and 54 eV, respectively [18]



map band structures in a three-dimensional k -space with angle-resolved photoelectron spectra, not only with linearly but also circularly/elliptically polarized light, and to obtain direct three-dimensional spin texture. Performing measurements of this kind on one sample prepared in the same UHV system gives complete information about the magnetism derived from the orbital angular momentum and spin.

The DEMETER beamline (Dual Microscopy and Electron Spectroscopy Beamline) has operated since the fall of 2021 and is dedicated to variable-polarization soft X-ray studies with advanced photoemission experiments. The Elliptically Polarized Undulator EPU can deliver linearly polarized light in any direction, as well as circularly polarized light (left- or right-handed). The DEMETER beamline consists of two separated branches, ending with two x-ray microscopes: photoemission electron microscope (PEEM) and scanning transmission X-ray microscopy STXM [24, 25]. The parent institution for the PEEM end-station is the Jerzy Haber Institute of Catalysis and Surface Chemistry of the Polish Academy of Sciences (ICSC PAS). The PEEM microscope has become a widely used technique for direct imaging of surfaces and interfaces. Chemical, magnetic, and electronic contrast can be achieved through the use of well-known spectroscopy methods: X-ray absorption spectroscopy (XAS), X-ray photoelectron spectroscopy (XPS), and angle-resolved photoemission spectroscopy (ARPES). The first method combined with variable polarization of the photon beam is widely used for imaging magnetic domains on a magnetic surface using X-ray magnetic circular dichroism (XMCD) and X-ray magnetic linear dichroism (XMLD) [26–28]. An additional advantage of the microscope is the ability to perform measurements at extreme temperatures in the range of 100–2000 K.

The second branch of the DEMETER beamline is equipped with a scanning transmission X-ray microscope (STXM). STXM microscopy is a method for obtaining a microscopic image of a sample (raster scanned) by detecting the intensity of X-rays transmitted through the sample. The end-station provides imaging techniques at room temperature and operates down to 10^{-6} mbar, but can also be backfilled with helium up to ambient pressure. The STXM mode uses a photomultiplier tube detector or a silicon drift fluorescence detector and is limited in resolution by the spot size of the illumination down to 30 nm [29].

ASTRA (Absorption Spectroscopy beamline for Tender energy Range and Above) is a bending magnet beamline currently opening for user operation. The beamline is built as an international collaboration of SOLARIS with Hochschule, the Institute of Physics at Bonn University, and the Synchrotron Light Research Institute (Thailand). It was explicitly designed as a beamline for X-ray absorption spectroscopy (XAS) and related techniques at tender and higher X-ray energies (range ~ 1 –15 keV) [30]. Besides

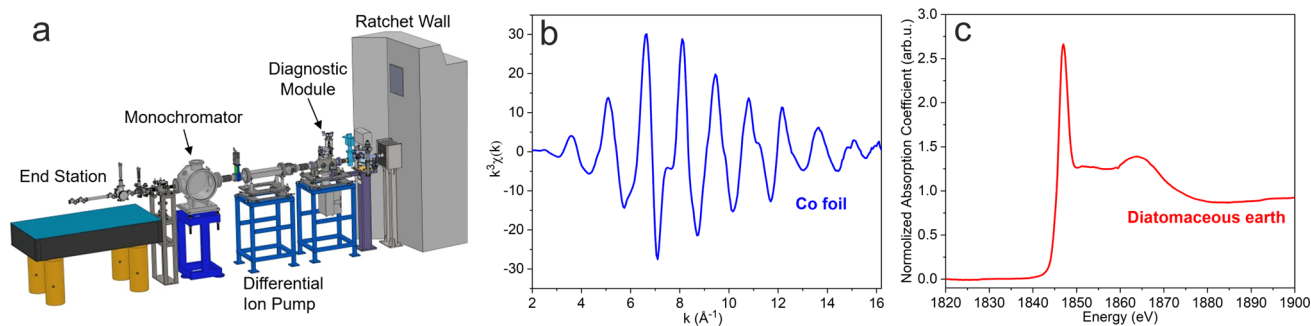


Fig. 5 ASTRA beamline details and experimental results. **a** Main beamline components downstream from SOLARIS radiation shield wall; **b** Co K-edge EXAFS spectrum measured at the ASTRA beamline and **c** Si K-edge XANES spectrum

the X-ray monochromator, the beamline does not have additional optical components such as lenses or mirrors and can be operated without radiation safety hatches (Fig. 5a). The beamline enables “standard” absorption measurements, i.e. recording XANES/EXAFS data at K-edges of elements starting from Na, Mg, Al and Si up to 3d metals. The energy range of ASTRA also includes L-edges of elements up to Bi and some M-edges of elements including uranium, which allows for the investigation of a variety of highly application-relevant materials. Measurements will be possible in the transmission, fluorescence, and surface-sensitive total electron yield mode. A compact vacuum X-ray spectrometer for high-energy resolution fluorescence detection was recently installed for experiments requiring higher spectral sensitivity. Moreover, in the next few years, the development of an optimized infrastructure for in situ and operando experiments and combinations of XAS with complementary techniques (e.g. mass spectrometry, UV–VIS, and IR spectroscopy) will be implemented.

SOLARIS provides users with services not only through the beamlines but also with complementary installations located at the Centre, e.g. the cryogenic electron microscopes (Cryo-EM) operating since 2019. In its three-year history, the Cryo-EM facility has become a fully operational centre for cryo-electron microscopy, working with researchers from Poland and across central and eastern Europe. The facility gives access to two high-end cryo-electron microscopes, i.e. Glacios and Krios G3i (both from Thermo Fisher Scientific). Glacios is fully dedicated to measurements at liquid nitrogen temperatures and is equipped with two cameras allowing micro-electron diffraction experiments or high- and low-dose imaging. The available system allows for obtaining density maps with a resolution of less than 3 Å for average and big particles (400 kDa and more) and 4–5 Å for small particles (less than 200 kDa). The second microscope, Titan Krios G3i, is equipped with a very flexible three-condenser lens system and constant power lens optics, which in combination with a field emission gun (FEG) electron emitter allows very stable high-resolution imaging. Two direct electron detectors assure fluent workflow and high throughput of any single-particle analysis or cryo-electron tomography experiment. The combination of microscope and detector properties allows getting the acquisition rate of more than 700 images per hour and by this good quality dataset over a single night of collection. Cryo-EM allowed for the performing of first-class research related to a number of biomedical projects. Strong examples of such studies are, among others, the design of new artificial protein cages published by K. Majsterkiewicz et. al. [31], new types of antibiotic mechanisms by D. Ghilarov et. al. [32], virus-like particles for cancer diagnostic and therapy by M. Ruzskowski et. al. [33] or programable virus-like particles for new vaccines by A.P. Biela [34].

It is worth mentioning that SOLARIS explores the potential for the industrial use of the available beamlines and the cryo-EM facility. Because of its unique status as the only synchrotron light source in central and eastern Europe, SOLARIS has the potential to become the leading applied research facility in the region. However, as evidenced by the experiences of other facilities, industry cooperation is linked to specific challenges and requires a comprehensive approach. In general, academic users of synchrotron radiation facilities have the necessary expertise to plan the experiments, perform the measurements semiautonomously, with limited support from beamline scientists, and perform a complete data analysis.

Industrial users, on the other hand, often face timely and economical restrictions when training in measurement techniques that may often be perceived as overly theoretical for application-related questions. Limited resources available for experiment planning and advanced data analysis lead to a situation with significant growth potential for the adaptation of synchrotron radiation for industrial applications. However, synchrotron radiation might be used for a wide field of economic activity, such as production, quality control, or research and development. Therefore, an Industry Liaison Office was recently created at SOLARIS, to overcome the barriers for industrial users, increase the share of applied research experiments at the facility, and provide a comprehensive service for our partners.

3 Technological development

3.1 Accelerator development

The SOLARIS accelerators are under permanent development. Recent work concentrates on the design and installation of new diagnostic instrumentation such as fast orbit feedback, a bunch-by-bunch feedback system, filling pattern, bunch length monitors, etc. Since the storage ring still possesses several free straight sections, various insertion devices are planned for new experimental beamlines along with optimizations of the storage ring optics in the near future. To meet the expectations of the users, new modes of operation are being considered and developed, i.e. single bunch and/or camshaft mode, and bunch compression modes for operation with short bunches. Moreover, currently, part of the work is focused on the new linac design delivering a low-emittance, compressed and full-energy (1.5 GeV) beam to the storage ring. The injector upgrade will allow for a top-up injection development together with a new injection scheme that will be transparent to the users. Additionally, it will open the possibility to accommodate a free electron laser (FEL).

3.2 Upgrades of existing infrastructure.

SOLARIS has the potential to become a significant research facility for measuring the electronic band structure of advanced materials with high angle, energy, and spin resolution in a wide energy range. Two beamlines, URANOS and PHELIX, producing high-quality synchrotron light, see their scientific future with the use of 3D spin detectors [35], but each of these beamlines has opted for a slightly different solution for complementary applications. PHELIX aims at VLEED (Very Low-Energy Electron Diffraction) spin detector determining two spin components and combining them with the spin rotator to detect the third spin component. URANOS will deliver two VLEED spin detectors orthogonally oriented to obtain full information about the spin of photoelectrons. Considering the different energy ranges of both beamlines (8–150 eV for URANOS and 50–1500 eV for PHELIX), they will constitute two complementary research devices. The STXM microscope is planned to be upgraded with the ptychography option. Ptychography is a method to reconstruct the structure (image) of a specimen from the diffraction patterns obtained from each point (area) scanned over a specimen using a convergent probe so that a part of the illuminated area overlaps. Ptychography reconstructs both the amplitude and phase of the scattered X-ray field and offers wavelength-limited resolution [36]. The Ptychography mode will use a pixel detector, a fast soft X-ray CMOS camera with the sample to be positioned out of focus to adjust the illumination spot size and the overlap. Additionally, STXM will have the possibility for electrochemical experiments. The electrochemical cell is currently being delivered and is going to be set in operation in the following months. The setup will allow for mapping of catalytic processes with spatial, elemental, and chemical sensitivity at real operating chemical conditions.

3.3 Beamlines under construction

The PolyX beamline is a compact bending magnet beamline for X-ray microimaging and X-ray microspectroscopy in the hard X-ray energy range (4–15 keV) and is expected for full user operation in 2024. PolyX comes from polycapillary X-ray optics that will be used for efficient X-ray focusing and from the possibility of using polychromatic X-rays to increase the rather low flux from the SOLARIS bending magnet in the hard X-ray energy range. The main experimental techniques will be X-ray microradiography and microtomography μ CT (absorption and phase contrast), X-ray fluorescence imaging (μ XRF) and spatially resolved X-ray absorption (μ XAS) and emission (μ XES) spectroscopy. Therefore, PolyX will enable imaging of the 2D and 3D structure, elemental distribution, and chemical phases in the investigated samples. In contrast to most SOLARIS beamlines, PolyX will focus on experiments that can be performed in air, and the beamline will be easy to reconfigure. In addition, a dedicated area for user-designed and test experiments will be provided in the experimental hutch. The white beam will also be available routinely. The spatial resolution in scanning experiments will be limited to $\sim 10 \mu\text{m}$ at 10 keV in the case of polycapillary optics and to $\sim 2 \mu\text{m}$ for ellipsoidal monocapillary optics. The spatial resolution of parallel beam X-ray absorption and phase contrast imaging will be limited to $\sim 1 \mu\text{m}$. PolyX will take advantage of two recent methodological advances. First, 3D X-ray multibeam microscopy with polycapillary optics [37, 38] will increase the imaging resolution to approximately 300 nm. Second, energy-dispersive X-ray absorption and emission spectroscopy with polycapillary optics and von Hamos spectrometers will enable time-resolved studies [39].

The CIRI (Chemical Infrared Imaging) beamline is currently under construction and has been designed to offer the best IR imaging capabilities available today. An M1 slotted mirror mounted on a moving arm will be inserted from the side of a modified dipole chamber. This position allows gathering both the bending magnet and edge radiation generated at the first achromat section just after a straight section. A set of several mirrors will be employed to deliver IR beam to the end-stations, additionally correcting for source aberrations with tangential and conical mirrors. The beam covering $4000\text{--}2 \text{ cm}^{-1}$ spectral range will be split into two branches, each able to again split the beam in two, giving a total of four potential end-stations. The first one will be a classical FT-IR microimaging system, but will also allow full-field imaging (with a focal plane array) at very small pixel projection sizes (around $1 \mu\text{m}$) and equipped with a bolometer detector reaching Far-IR spectral range. The second station will be dedicated to nanoscale imaging via AFM-based techniques. A system capable of scattering scanning near-field optical microscopy (s-SNOM) and photothermal expansion microscopy will be coupled to the synchrotron beam and will offer imaging with chemical contrast

at the 10–20 nm spatial resolution. s-SNOM as a surface technique (5–10 nm probing depth) is very well suited for 2D materials analysis, photonics, polaritonics, but can also be applied to biological samples. Finally, the third end-station will enable optical photothermal infrared imaging (O-PTIR), which enables chemical imaging with optical spatial resolution at around 400 nm, but with less restrictive sample requirements. The backscattering geometry allows for easy measurements and probing using a 532 nm laser is compatible with live-cell imaging. Moreover, a Raman spectroscopy detector module will be coupled to the O-PTIR station, allowing simultaneous IR and Raman measurements of samples, with microplastic and cultural heritage samples as a focus. The set of four different experimental techniques will enable measurements of many samples from centimetre-to nanometer-scale size and spatial resolution.

SOLCRYS (SOLARIS crystallographic beamline) is a beamline dedicated to X-ray diffraction experiments. This project involves the construction of a beamline suited for single-crystal diffraction studies, in particular, for protein crystallography. The radiation source proposed for SOLCRYS beamline is a 3-Tesla wiggler, which will be located at the second straight section of SOLARIS' storage ring. The X-ray optics are based on a standard combination of two mirrors and a cryogenically cooled double crystal monochromator (DCM/DMM) (adjustable Si(111) crystals and Mo/B4C multilayers). The energy resolution ($\Delta E/E$) is aimed to be about 1.5×10^{-4} for DCM (high-resolution mode) and 1×10^{-2} for DMM (high flux mode). The expected diameter of the focused beam will be less than 100 μm with X-ray flux better than 10^{11} photons/sec. It is assumed that the SOLCRYS end-station will be equipped with a setup for standard crystallographic measurements, serial screening experiments, and data collection in a helium atmosphere. Full automation of measurements is assumed, using an automatic, sample-changing system (a robotic arm with magnetic gripper) integrated with a high-precision diffractometer and microscopic system. Full automation of diffraction experiments will also include remote access via the Internet to the X-ray data collection system. Moreover, charge-density studies and high-pressure experiments will also be possible.

3.4 Beamlines in the conceptual design phase

Currently, two additional beamlines are under conceptual design and discussed with potential users. The first one will aim at providing high-energy resolution X-ray spectroscopy schemes for X-ray absorption and X-ray emission measurements. Additionally, surface-sensitive techniques, such as grazing incidence and grazing exit geometries, are envisaged. The beamline will be dedicated to materials science and chemistry applications and will operate in a tender and hard X-ray range.

The second project aims at the construction of a beamline dedicated to small-angle X-ray scattering (SAXS) studies. This planned beamline will offer an experimental setup suited to study the microstructure, order, and orientation in various materials. The scope of research applications of such a beamline will be very wide, ranging from studies of the structure of biological systems (proteins, nucleic acids, and lipid systems) in solution, through the study of polymers, liquid crystals, nanoparticles, and drug delivery systems, and ending with typical solid-state samples (glasses, alloys, molecular sieves, etc.). This project will be located in a new experimental hall and complement other structural methods available at SOLARIS, particularly cryo-electron microscopy, primarily used to study biomedical systems. If these projects receive a positive assessment and qualify for funding, the first user experiments at these stations are envisaged for 2026.

4 Perspective and scientific challenges

The SOLARIS Centre aims at delivering a unique research infrastructure allowing for conducting experiments with a range of experimental methods to be applied in the research field of natural sciences, engineering, and technical sciences. It can be concluded that SOLARIS will allow interdisciplinary and multidisciplinary studies with a particular focus on research essential for a modern and green society, research at molecular and structural levels on systems important for new drugs and in the area of civilization diseases, testing modern materials in the field of renewable sources and energy storage, and developing innovative solutions for science and digital technologies. A few of the many examples of scientific challenges to be addressed at SOLARIS are presented in this section.

One of the essential research directions, which will be addressed in the future at SOLARIS, is the possibility of conducting material examinations in chemistry, photocatalysis, and artificial photosynthesis. Despite all the scientific advances in recent decades, it remains a significant challenge to construct a device capable of producing solar fuels, such as hydrogen, in large quantities and at a price that can compete with fossil fuels. Therefore, much research will focus on the atomic and structural modification of materials important for catalysis or artificial photosynthesis processes. These materials are known to be useful for the use of photosensitizers (molecular dyes) capable of absorbing sunlight and transferring electrons to the conduction band in a semiconductor [40]. These hybrid systems have higher efficiency, but research is still needed to improve the charge transfer efficiency and photostability and increase the cross sections for absorption in the optical range. Another catalyst important for investigations is the hybrid system based on metallic nanoparticles with the d^{10} electron system, which absorb light very efficiently as a result of surface plasmon resonance [41]. Despite the very advanced research and development in the field of plasmonic materials, there is still a lack of knowledge about the processes leading to charge transfer, the influence of the metal–semiconductor junction on the performance of the system, and many other parameters. We should emphasize that the energy and climate crisis is inextricably linked to the use of fossil fuels and

greenhouse gas emissions. Therefore, it is not surprising that scientists are interested in the search for new technologies and solutions in the field of catalysis that will allow them to respond to the energy and environmental challenges of the modern world. However, the synthesis of novel and environmentally friendly catalytic materials with improved properties, i.e. higher activity, selectivity, and stability, is a very complex and time-consuming task. This is due to the complexity of the inherently dynamic catalytic processes and a large number of properties that determine the performance of the material, such as composition, type of substrate, particle size, and type of active centres. Understanding the details of the substrate-product transformation during the catalytic process and the relationship between the catalyst structure and reactivity is necessary. Ex situ characterization techniques still dominate the typical approach for gaining insight into catalytic reaction mechanisms, often performed under conditions that differ significantly from actual catalyst operating conditions and do not provide complete data on catalyst-reactant interactions. Therefore, the research on catalysts is moving towards the research in the operando mode, i.e. research under actual "working conditions" of the active catalyst [42].

Another area of research addresses the molecular and structural levels of systems important for new drug development and the area of civilization diseases. According to statistics, the number of new cancer cases in Poland will increase in the coming years for both men and women [43]. Despite the rapid development of modern methods of fighting cancer, chemotherapy remains one of the most important, and in the case of some cancers, the only treatment method. A well-defined way of interacting molecular complexes with the DNA structure, related to the chemical structure and mechanisms of interaction, will help in the design of more effective drugs. Furthermore, dedicated approaches will be investigated to understand the microenvironment of cancer with the aim, for example, to create label-free, nondestructive, and highly accurate comprehensive histopathological models of pancreatic and breast cancers using machine learning. Simultaneously, appropriate experimental approaches for biomedical sample preparation and nanoscale measurements have to be developed to address new challenges for the characterization of single cells or biomaterials. Studies will also explore the influence of a range of nanomaterials on the structure of model biomembrane systems based on different derivatives.

In the area of imaging and microscopy research, methodological developments related to the plenoptic X-ray imaging modality are planned. In X-ray plenoptic microscopy [44, 45] a sample is illuminated by multiple beamlets from a polycapillary device at slightly different viewing angles. By means of numerical reconstruction, tomographic slices of the sample can be visualized from a single X-ray exposure. Recently an X-ray plenoptic microscope with absorption and phase contrast and sub-micrometre spatial resolution has been demonstrated using radiation from an X-ray tube [37, 46]. Transfer and adaptation of the X-ray plenoptic microscope to the PolyX beamline will result in a 100–1000 fold intensity increase and will enable routine experiments with this unique technique.

Finally, we should mention that SOLARIS, like other synchrotron facilities, is a unique laboratory device enabling data analysis based on artificial intelligence techniques [47]. A vital aspect of the facility is its multimodality, which will provide scientists with very flexible experimental conditions that allow measurements in unique configurations. Due to the complexity of the experimental conditions and in order to avoid additional system optimization and trial and error measurements, experimental data analysis can be supported by computer processing tools and particularly machine learning models [48, 49]. Machine learning will allow for automatic optimization of experimental conditions and it will enable the analysis of experimental data in the context of determining and learning about the studied biological or chemical mechanisms. Currently, it is one of the fastest-growing fields of technology, driven not only by the development of new algorithms but also by the availability of enough data to start self-learning mechanisms. Therefore, the fields of machine learning and artificial intelligence will be explored very intensively in the following years of SOLARIS operation.

Acknowledgements We acknowledge the initial investment for the SOLARIS National Synchrotron Radiation Centre covered by the European Union (European Regional Development Fund) and the national budget under the Innovative Economy Operational Programme and the Ministry of Education and Science for funds related to beamlines construction. Operational costs of SOLARIS NSRC are covered by the Ministry of Education and Science under the Agreement: 1/SOL/2021/2. The ASTRA beamline was partly funded within the project "Innovative Hochschule–Leuchtturm NR-Aus der Höhe in die Breite" (03-IHS-084) by the German Federal Ministry of Education and Research, and its further development for measuring at low photon energies and with high-energy resolution fluorescence detection is supported within the EU Horizon2020 program (952148-Sylinda).

Data availability Data sharing does not apply to this article as no data sets were generated or analysed during the current study.

Open Access This article is licensed under a Creative Commons Attribution 4.0 International License, which permits use, sharing, adaptation, distribution and reproduction in any medium or format, as long as you give appropriate credit to the original author(s) and the source, provide a link to the Creative Commons licence, and indicate if changes were made. The images or other third party material in this article are included in the article's Creative Commons licence, unless indicated otherwise in a credit line to the material. If material is not included in the article's Creative Commons licence and your intended use is not permitted by statutory regulation or exceeds the permitted use, you will need to obtain permission directly from the copyright holder. To view a copy of this licence, visit <http://creativecommons.org/licenses/by/4.0/>.

References

1. A.I. Wawrzyniak, C.J. Bocchetta, S.C. Leemann, and S. Thorin, *Proc. IPAC'11*, San Sebastian, Spain, THPC123 3173–3175 (2011)
2. A.I. Wawrzyniak, A. Marendziak, A. Kisiel, P. Borowiec, R. Nietubyć, J. Wiechecki, K. Karaś, K. Szamota-Leandersson, M. Zając, C.J. Bocchetta, M.J. Stankiewicz, *Nucl. Instrum. Methods. Phys. Res. B* **411**, 4–11 (2017). <https://doi.org/10.1016/j.nimb.2016.12.046>

3. A.I. Wawrzyniak, R. Panaś, A. Curcio, M. Knafel, G. Kowalski, A. Marendziak, Nucl. Instrum. Methods. Phys. Res. B **493**, 19–27 (2021). <https://doi.org/10.1016/j.nimb.2021.01.020>
4. Synchrotron Radiation in Natural Science 20 (2020)
5. M. Zajac, T. Giela, K. Freindl, K. Kollbek, J. Korecki, E. Madej, K. Pitala, A. Koziol-Rachwał, M. Sikora, N. Spiridis, J. Stepień, A. Szkudlarek, M. Ślęzak, T. Ślęzak, D. Wilgocka-Ślęzak, Nucl. Instrum. Methods. Phys. Res. B **492**, 43–48 (2021). <https://doi.org/10.1016/j.nimb.2020.12.024>
6. A. Plewa, A. Kulka, E. Hanc, J. Sun, M. Nowak, K. Redel, Lu. Li, J. Molenda, Adv. Funct. Mater. **294**, 2102406 (2021)
7. D. Rybicki, M. Sikora, J. Stepień, Ł. Gondek, K. Goc, T. Strączek, M. Jurczyszyn, C. Kapusta, Z. Bukowski, M. Babij, M. Matusiak, M. Zajac, Phys. Rev. B **102**, 19 (2020). <https://doi.org/10.1103/PhysRevB.102.195126>
8. M. Ślęzak, T. Ślęzak, P. Drózdź, B. Matlak, K. Matlak, A. Koziol-Rachwał, M. Zajac, J. Korecki, Sci. Rep. **9**, 889 (2019). <https://doi.org/10.1038/s41598-018-37110-8>
9. A. Koziol-Rachwał, M. Ślęzak, M. Zajac, P. Drózdź, W. Janus, M. Szpytma, H. Nayyef, T. Ślęzak, APL Mater. **8**, 061107 (2020). <https://doi.org/10.1063/5.0011736>
10. M. Ślęzak, P. Drózdź, W. Janus, M. Szpytma, H. Nayyef, A. Koziol-Rachwał, M. Zajac, T. Ślęzak, J. Magn. Magn. Mater. (2022). <https://doi.org/10.1016/j.jmmm.2021.168783>
11. M. Ślęzak, P. Drózdź, W. Janus, H. Nayyef, A. Koziol-Rachwał, M. Szpytma, M. Zajac, T.O. Menteş, F. Genuzio, A. Locatelli, T. Ślęzak, Nanoscale **12**(35), 18091–18095 (2020). <https://doi.org/10.1039/D0NR04193A>
12. M. Ślęzak, H. Nayyef, P. Drózdź, W. Janus, A. Koziol-Rachwał, M. Szpytma, M. Zajac, T.O. Menteş, F. Genuzio, A. Locatelli, T. Ślęzak, Phys. Rev. B **104**, 134434 (2021). <https://doi.org/10.1103/PhysRevB.104.134434>
13. A. Koziol-Rachwał, M. Szpytma, N. Spiridis, K. Freindl, J. Korecki, W. Janus, H. Nayyef, P. Drózdź, M. Ślęzak, M. Zajac, T. Ślęzak, Appl. Phys. Lett. **120**, 072404 (2022). <https://doi.org/10.1063/5.0082729>
14. B.A. Bernevig, C. Felser, H. Beidenkopf, Nature **603**, 7899 (2022). <https://doi.org/10.1038/s41586-021-04105-x>
15. K. Nowak, M. Jurczyszyn, M. Chrobak, K. Maćkosz, A. Naumov, N. Olszowska, M. Rosmus, I. Miotkowski, A. Kozłowski, M. Sikora, M. Przybylski, Materials **15**, 2083 (2022). <https://doi.org/10.3390/ma15062083>
16. A. Ptok, M. Rosmus, N. Olszowska, Electronic band structure of FeBi₂Te₄—in preparation
17. M. Weis, K. Balin, B. Wilk, T. Sobol, A. Ciavardini, G. Vaudel, V. Juvé, B. Arnaud, B. Ressel, M. Stupar, K.C. Prince, G. De Ninno, P. Ruello, J. Szade, Phys. Rev. B **104**, 245110 (2021). <https://doi.org/10.1103/PhysRevB.104.245110>
18. J. Sitnicka, K. Park, P. Skupiński, K. Graszka, A. Reszka, K. Sobczak, J. Borysiuk, Z. Adamus, M. Tokarczyk, A. Avdonin, 2D Mater. **9**, 015026 (2022). <https://doi.org/10.1088/2053-1583/ac3cc6>
19. I.I. Klimovskikh, M.M. Otrikov, D. Estyunin, S.V. Eremeev, S.O. Filnov, A. Koroleva, E. Shevchenko, V. Voroshnin, A.G. Rybkin, I.P. Rusinov, M. Blanco-Rey, M. Hoffmann, Z.S. Aliev, M.B. Babanly, I.R. Amirasanov, N.A. Abdullayev, V.N. Zverev, A. Kimura, O.E. Tereshchenko, K.A. Kokh, L. Petaccia, G. Di Santo, A. Ernst, P.M. Echenique, N.T. Mamedov, A.M. Shikin, E.V. Chulko, npj Quantum Mater. **5**, 54 (2020). <https://doi.org/10.1038/s41535-020-00255>
20. M. Szczepanik-Ciba, T. Sobol, J. Szade, Nucl. Instrum. Methods. Phys. Res. B **492**, 10 (2020). <https://doi.org/10.1016/j.nimb.2021.01.021>
21. B. Lv, T. Qian, H. Ding, Nat. Rev. Phys. **1**, 10 (2019). <https://doi.org/10.1038/s42254-019-0088-5>
22. X.I. Pereira-Hernández, A. DeLaRiva, V. Muravev, D. Kunwar, H. Xiong, B. Sudduth, M. Engelhard, L. Kovarik, E.J.M. Hensen, Y. Wang, A.K. Datye, Nat Commun **10**, 1358 (2019). <https://doi.org/10.1038/s41467-019-09308-5>
23. V.A. Saveleva, V. Papaefthimiou, M.K. Daletou, W.H. Doh, C. Ulhaq-Bouillet, M. Diebold, S. Zafeirotas, E.R. Savinova, J. Phys. Chem. C **120**, 29 (2016). <https://doi.org/10.1021/acs.jpcc.5b12410>
24. T.O. Menteş, G. Zamborlini, A. Sala, A. Locatelli, Beilstein J. Nanotechnol. (2014). <https://doi.org/10.3762/bjnano.5.198>
25. L. Aballe, M. Foerster, E. Pellegrin, J. Nicolas, S. Ferrer, J. Synchrotron Radiat. **22**, 3 (2015). <https://doi.org/10.1107/S1600577515003537>
26. J. Feng, A. Scholl, in Science of Microscopy, ed By P. W. Hawkes, J. H. C. Spence 2007 657 https://doi.org/10.1007/978-3-030-00069-1_10
27. Th. Schmidt, S. Heun, J. Slezak, J. Diaz, K.C. Prince, G. Lilienkamp, E. Bauer, Surf. Rev. and Lett. **5**, 6 (1998). <https://doi.org/10.1142/S0218625X98001626>
28. T.O. Menteş, A. Locatelli, J. Electron Spectrosc. Relat. Phenom. (2012). <https://doi.org/10.1016/j.elspec.2012.07.007>
29. L. Lühl, K. Andrianov, H. Dierks, A. Haidl, A. Dehlinger, M. Heine, J. Heeren, T. Nisius, T. Wilhein, B. Kanggießer, J Synchrotron Radiat. **26**(2), 430–438 (2019). <https://doi.org/10.1107/S1600577518016879>
30. J. Hormes, W. Klysubun, J. Göttert, H. lichtenberg, A. Maximenko, K. Morris, P. Nita, A. Prange, J. Szade, L. Wagne, M. Zajac, Nucl. Instrum. Methods Phys. Res. B **489**, 76–81 (2021)
31. K. Majsterkiewicz, A.P. Biela, S. Maity, M. Sharma, B. Piette, A. Kowalczyk, S. Gawel, S. Chakraborti, W.H. Roos, J. Heddle, Nano Lett. **22**, 8 (2022). <https://doi.org/10.1021/acs.nanolett.1c04222>
32. D. Ghilarov, S. Inaba-Inoue, P. Stepien, F. Qu, E. Michalczyk, Z. Pakosz, N. Nomura, S. Ogasawara, G.C. Walker, S. Rebuffat, S. Iwata, J.G. Heddle, K. Beis, Molecular mechanism of SbmA, a promiscuous transporter exploited by antimicrobial peptides. Sci. Adv. **7**(37), eabj5363 (2021). <https://doi.org/10.1126/sciadv.abj5363>
33. M. Ruskowski, A. Strugala, P. Indyka, G. Tresset, M. Figlerowicz, A. Urbanowicz, Nanoscale **14**(8), 3224–3233 (2022). <https://doi.org/10.1039/D1NR05650F>
34. A.P. Biela, A. Naskalska, F. Fatehi, R. Twarock, J.G. Heddle, Commun. Mater. **3**, 7 (2022). <https://doi.org/10.1038/s43246-022-00229-3>
35. R. Bertacco, F. Ciccacci, Oxygen-induced enhancement of the spin-dependent effects in electron spectroscopies of Fe(001). Phys. Rev. B **59**, 6 (1999). <https://doi.org/10.1103/PhysRevB.59.4207>
36. A.P. Hitchcock, J. Electron. Spectrosc. Relat. Phenom. **200**, 49–63 (2015). <https://doi.org/10.1016/j.elspec.2015.05.013>
37. K.M. Sowa, M.P. Kujda, P. Korecki, Appl. Phys. Lett. **116**, 014103 (2020). <https://doi.org/10.1063/1.5131494>
38. K.M. Sowa, P. Korecki, Opt. Express **28**, 16 (2020). <https://doi.org/10.1364/OE.394262>
39. W. Błachucki, J. Czaplă-Masztafiak, J. Sá, J. Szlachetko, J. Anal. At. Spectrom. **34**, 7 (2019). <https://doi.org/10.1039/C9JA00159J>
40. B. O'Regan, M. Grätzel, Nature **353**(6346), 737–740 (1991). <https://doi.org/10.1038/353737a0>
41. D. Gramotnev, S. Bozhevolnyi, Nat. Photon. **2**, 83–91 (2010). <https://doi.org/10.1038/nphoton.2009.282>
42. A.I. Frenkel, J.A. Rodriguez, J.G. Chen, ACS Catal. **2**, 11 (2012). <https://doi.org/10.1021/cs3004006>
43. J. Didkowska, U. Wojciechowska, W. Zatoński, Centrum Onkologii Instytut im. Marii Skłodowskiej-Curie, Warszawa (2009).
44. K.M. Sowa, B.R. Jany, P. Korecki, Optica **5**, 5 (2018). <https://doi.org/10.1364/OPTICA.5.000577>
45. E. Longo, D. Alj, J. Batenburg, O. de La Rochefoucauld, C. Herzog, I. Greving, Y. Li, M. Lyubomirskiy, K. Vidar Falch, P. Estrela, S. Flenner, N. Viganò, M. Fajardo, and P. Zeitoun, Photonics **9**, 2, 98 (2022) <https://doi.org/10.3390/photonics9020098>
46. K.M. Sowa, P. Korecki, Opt. Express **28**, 23223–23238 (2020)
47. D. Liberda, M. Hermes, P. Koziol, N. Sone, T. Wrobel, J. Biophotonics **13**, 8 (2020). <https://doi.org/10.1002/jbio.202000122>

48. J. Kim, F. Ling, D. Plattenberger, A. Clarens, A. Lanzirotti, M. Newville, C. Peters, *Comput. Geosci.* **156**, 104898 (2021). <https://doi.org/10.1016/j.cageo.2021.104898>
49. J. Li, X. Huang, P. Pianetta, Y. Liu, *Nat. Rev. Phys.* **3**, 766–768 (2021)